

ON THE USE OF THERMOGRAPHIC TECHNIQUE TO DETERMINE THE FATIGUE LIMIT OF A COLD DRAWN CARBON STEEL

Bandeira C.F.C.⁽¹⁾, Kenedi P.P.⁽²⁾, Castro J.T.P.⁽³⁾, Meggiolaro M.A.⁽⁴⁾

^(1,2) Programa de Pós Graduação em Eng. Mecânica e Tecnologia de Materiais CEFET - Rio de Janeiro - Brazil, ⁽¹⁾ fillypebandeira@hotmail.com, ⁽²⁾ paulo.kenedi@cefet-rj.br

^(3,4) Departamento de Engenharia Mecânica PUC - Rio de Janeiro - Brazil

⁽³⁾ jtcatro@puc-rj.br, ⁽⁴⁾ meggi@puc-rj.br

ABSTRACT

An accelerated thermographic technique and classic procedures are used to measure the fatigue limit of a cold drawn SAE 1020 carbon steel, using a rotating bending machine. Material temperature variations for different stress amplitude levels are accessed using an infrared camera. To validate the fatigue limit obtained by thermography, it is compared to the limit obtained by the traditional Nixon's up-and-down technique. Experimental results confirm that the fast thermographic approach yields fatigue limits quite close to the much slower staircase technique, indicating that it can be really a major asset for practical applications.

KEYWORDS

Fatigue, Fatigue limit, Thermography, Staircase.

INTRODUCTION

The fatigue or endurance limit S_L is an important parameter for design purposes, since it establishes a material strength that supposedly can be used to avoid fatigue failures in practice. The fatigue limit obtained by testing small polished specimens can be modified to be used in the design or analysis of real structural components, considering modifying factors to account for the effects of surface finish and similar parameters that typically reduce it [1]. However other factors like compressive residual stresses or even coxing (fatigue strengthening due cycling loading close to S_L) can increase the fatigue limit [2-5].

Classic methods to obtain the fatigue limit require a large number of specimens, are laborious, time consuming, and quite expensive. Fortunately, new thermographic techniques have been recently developed to obtain fatigue limits in a much cheaper and fast way [6-13]. This method can be much more efficient than the standard up-and-down (or staircase) method, which has been traditionally used as a so-called accelerated method to determine the fatigue limit of materials, albeit it does not deserves this name. Thermography, on the other hand, is a really fast method to determine fatigue limits. The idea is to correlate the stress amplitude σ_a with the heat it generates on the specimen surface, since it can be used to determine the fatigue limit of materials through the location abrupt temperature variations induced by the transition between elastic and cyclic plastic strains, the cause for fatigue damage.

THE THERMOGRAPHIC TECHNIQUE

The thermographic technique is characterized by the use of thermo-elasticity principles to determine the fatigue limit. It assumes that fatigue failures in materials occur when the

plastic deformation energy reaches a constant value, characteristic of each material [7, 8]. This physically reasonable hypothesis allowed a rapid correlation between temperature increments and the number of loading cycles, since fatigue damage clearly is an energy dissipation process [9]. Figure 1 shows a typical temperature versus number of cycles curve obtained by thermographic techniques during a fatigue test.

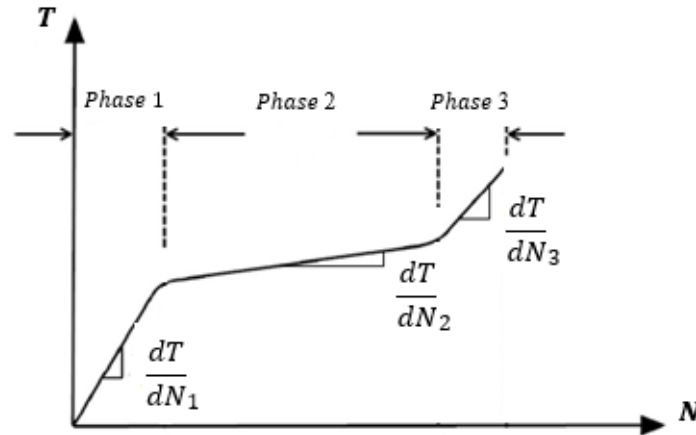


Figure 1: Typical N vs T relation observed at a critical point during a fatigue test.

Phases 1, 2, and 3 in Figure 1 represent the three thermal stages observed on the surface of a fatigue specimen during a typical thermographic fatigue test. These stages can be associated to the fatigue process, with phase 1 representing the crack nucleation, phase 2 the crack propagation, and phase 3 the imminent sudden failure. Depending on the stress level, the $T \times N$ curves typically translate on both the T and N axes, reducing the temperature variations and increasing the number of cycles to failure as σ_a approaches S_L . If $\sigma_a < S_L$, the temperature does not change or changes very little, generating $dT/dN_1 = dT/dN_2 = dT/dN_3 \sim 0$, indicating no fatigue damage generation.

From the typical behavior of $T \times N$ curves, Risitano et al. [7-8, 10] proposed to determine the fatigue limit in a very fast way by evaluating only their phase 1 for several stress amplitudes, using a single specimen to plot $\sigma_a \times \Delta T_1$ or $\sigma_a \times dT/dN_1$, where ΔT_1 is the temperature variation at the end of phase 1. The behavior of $\sigma_a \times \Delta T_1$ or $\sigma_a \times dT/dN_1$ curves typically has a bilinear trend with different slopes, and the fatigue limit is determined by the intersection between the curve with highest slope with the σ_a -axis, when $\Delta T_1 = 0$ or $dT/dN_1 = 0$.

EXPERIMENTAL RESULTS

The material characterization was done by its chemical composition and by tensile tests. The specimen geometry was defined according to ASTM E466-15 [14]. The fatigue tests were performed in a rotating bending machine RBF 200 with a test frequency around 8500rpm ($\approx 141\text{Hz}$). The traditional up-and-down sequential tests considered $5 \cdot 10^6$ cycles as a suitable life to characterize the classic fatigue limit of steels, and the thermography tests were performed using the temperature increasing rate of phase 1 to determine the fatigue limit.

Material Characterization and Specimen Definition

The material used in this research is a carbon steel SAE 1020, obtained by a cold drawn manufacturing process. Table 1 shows this material chemical composition and Table 2 its tensile mechanical properties.

Table 1: Chemical Composition

| C | Si | Mn | P | S | Cr | Ni | Mo | Al | Cu | Ti | Nb | V |
|-------|-------|-------|-------|--------|-------|-------|-------|-------|-------|--------|--------|-------|
| 0,226 | 0,114 | 0,510 | 0,020 | 0,0028 | 0,024 | 0,011 | 0,003 | 0,017 | 0,026 | <0,001 | <0,003 | 0,001 |

Table 2: Tensile Mechanical Properties

| Specimen number | S_y (MPa) | S_{UT} (MPa) | EL (%) | AR (%) |
|-----------------|-------------|----------------|----------|----------|
| 1 | 590 | 680 | 14,5 | 48,50 |
| 2 | 535 | 635 | - | 51,50 |
| 3 | 605 | 685 | - | 50,50 |

S_y is the yield strength, S_{ut} is the ultimate strength, $EL(\%)$ is the elongation and $AR(\%)$ is the area reduction. The flow stress, or the mean value of S_y (575 MPa) and S_{ut} (665 MPa), was used in initial fatigue tests to adjust and calibrate the test machine. Manufacturing precautions were taken in order to guarantee the data repeatability and reliability, as recommended by ASTM E466-15 standard. The test specimens have a mean roughness $R_a = 0.78 \mu m$. Figure 2 shows the fatigue test specimens dimensions.

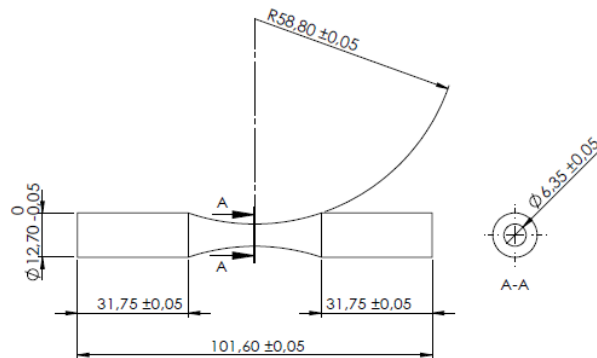


Figure 2: Specimen geometry

The stress amplitude steps used in the classic up-and-down tests (either to increase or to decrease the load in subsequent tests after a failure or a survival, respectively) was $s = \sigma_a/S_{ut} = 2\%$. The first value of σ_a/S_{ut} was an educated guess of 40%, based on the relatively high material tensile strength and on its good surface finish. Figure 3 shows results obtained with from staircase method.

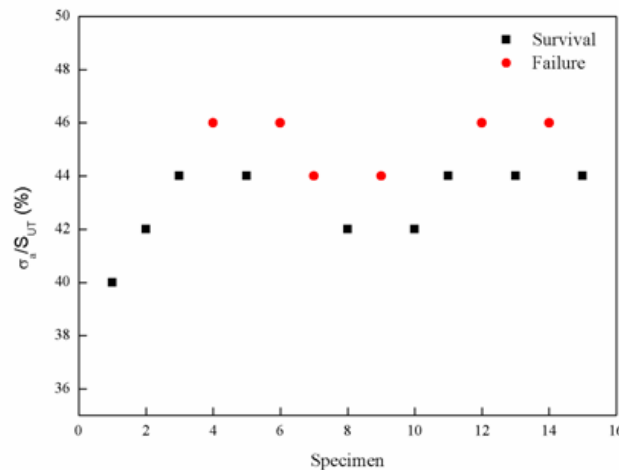


Figure 3: Staircase Results

These 15 test results have been statistically analyzed by Dixon's method [15], to determine the mean value (μ) and standard deviation (φ) of the fatigue limit measured by staircase approach (S_{LSC}), see Equation 1.

$$S_{LSC} = \mu \pm \varphi \rightarrow S_{LSC} = (44,3 \pm 2,4)\% \rightarrow S_{LSC} = (295,2 \pm 7,1)MPa \quad (1)$$

Thermographic Results

The specimen surface temperature variation was recorded in real time by a FLIR A320 infrared camera, with resolution of 320 x 240 pixels, data acquiring frequency of 30Hz, and temperature sensibility of 50mK. This thermographic camera, which is not cheap, but is not as expensive as fancier models either, proved to have enough resolution and accuracy to perform the required temperature measurements. In order to improve the camera performance, the middle surface of all fatigue specimens was black painted to increase their emissivity, as shown in Figure 4. In addition, a black cloth was used to cover the test machine and the infrared camera, to minimize the effect of unavoidable noise sources induced by the variable laboratory environment.



Figure 4: Black Painted Specimen

First, the camera was used to characterize the material temperature variations until the final fatigue failure induced by $\sigma_a/S_{ut} = 60\%$, 56% , 54% and 52% , to investigate the behavior of the three temperature phases and their associated increasing rates dT/dN . In the sequence, other stress amplitude levels were tested only until the start of phase 2, using always the same specimen. Finally, the curve σ_a vs dT/dN_1 was plotted to define the fatigue limit according to Risitano et al. method.

Figure 5 shows the curves $T_{max} \times N$ measured for each stress amplitude and Figure 6 shows some images extracted from the ResearchIR software during the fatigue test for $\sigma_a/S_{ut} = 60\%$.

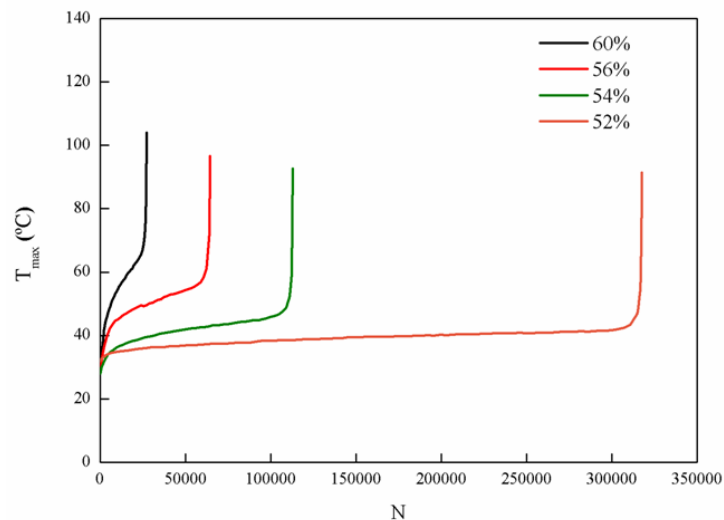


Figure 5: Relation N vs T_{max} .

Figure 5 shows that phase 1 is responsible for a small part of the total number of cycles reached for each stress amplitude until failure, as observed by *Fargione, et al* [8]. In addition, Figure 5 shows that the material behavior in phase 2 is not characterized by temperature stabilization, but by a relatively small constant temperature increase rate.

Figure 6 shows the temperature evolution for $\sigma_a/S_{ut} = 60\%$ during the entire fatigue test with pictures extracted from the ResearchIR software used by the FLIR camera to show the temperature field on the specimen surface. To determine the fatigue limit, the curves σ_a vs dT/dN_1 are plotted for all stress amplitude tested. Two curves are fitted to determine the fatigue transition region, with the abrupt slope changing. Figure 7 shows σ_a vs dT/dN_1 and the fitting curves.

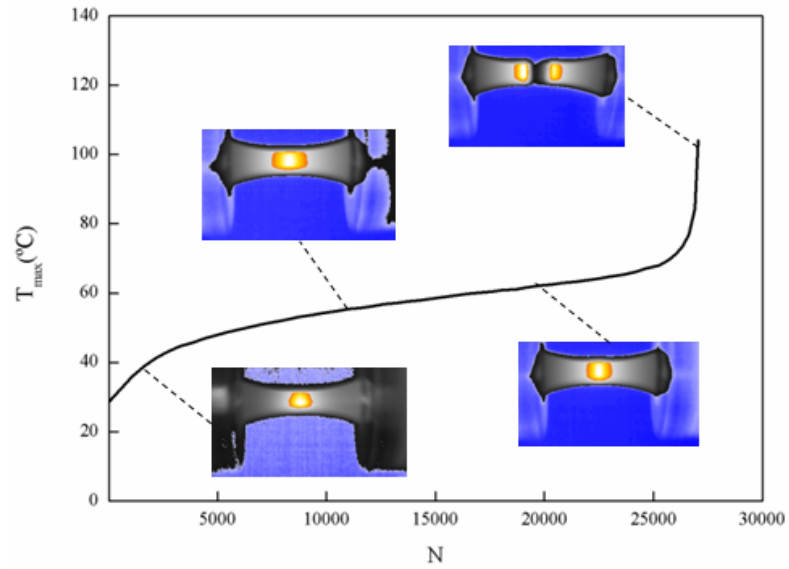


Figure 6: Relation N vs T_{max} - Temperature Evolution for $\sigma_a/S_{UT} = 60\%$.

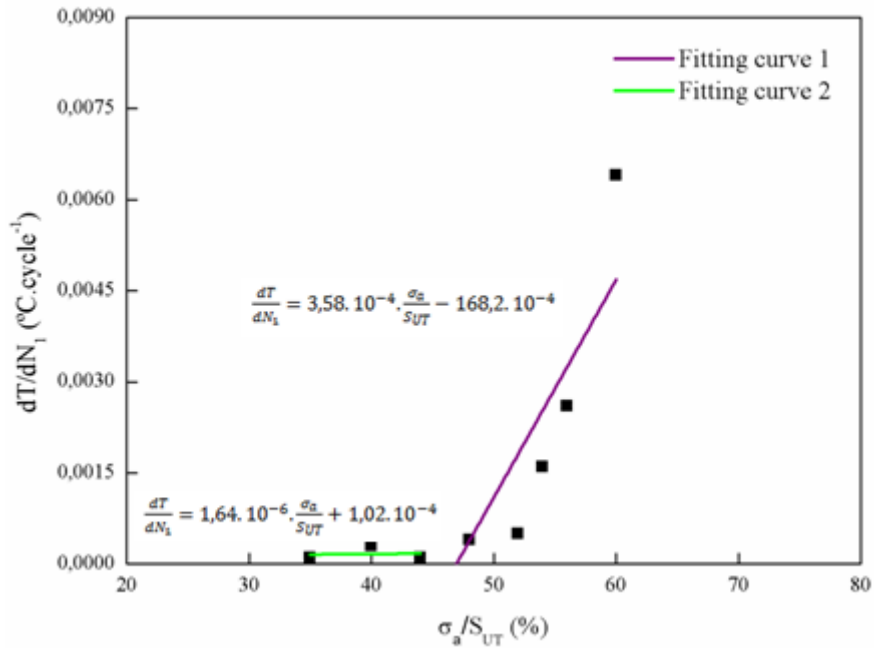


Figure 7: Fitting Curves

To determine the fatigue limit using the thermographic method ($S_{L_{TH}}$), the fitting curve 1 has to be prolonged until it crosses the σ_a -axis, where $dT/dN_1 = 0$.

$$0 = 3,58 \cdot 10^{-4} \cdot \frac{\sigma_a}{S_{UT}} - 168,2 \cdot 10^{-4} \quad (2)$$

$$\frac{\sigma_a}{S_{UT}} = S_{L_{TH}} = 46,9\% \quad (3)$$

DISCUSSION OF RESULTS

The fatigue limit determined by the classic up-and-down or staircase method based on fifteen specimens tested in a sequential way, following a pass or no-pass methodology, yielded a relatively small (for fatigue tests) standard deviation when compared to its mean value ($288,1\text{MPa} \leq S_{LSC} \leq 302,3\text{MPa}$), as calculated by Dixon's statistical tools, indicating a relatively homogeneous sample.

The fatigue limit determined by the thermographic method $S_{LTH} = 311,9\text{Mpa}$ was slight higher, but still close to value obtained by the much slower staircase method. The 8.3% difference between them is within the values observed by *La Rosa et al* [7].

CONCLUSION

The thermographic approach was used to determine the fatigue limit of a cold drawn steel SAE 1020, yielding a fatigue limit slight higher than the value obtained by the much slower and laborious up-and-down methodology, indicating it can indeed be used as a practical tool to measure such an important property in practical applications.

REFERENCES

- [1] Shigley, J.E.; Mishke, C.R.; Budynas, R.G. Mechanical Engineering Design, McGraw-Hill 2004.
- [2] Bathias, C.; Paris, P. C. Gigacycle fatigue in mechanical practice, Marcel Dekker, 2005.
- [3] Nicholas, T. High cycle fatigue – A mechanics of materials perspective, Elsevier 2006.
- [4] Pollak, R.; Palazotto, A.; Nicholas, T. A simulation-based investigation of the staircase method for fatigue strength testing. *Mech Mater* 38:1170-1181, 2006.
- [5] Castro, J.T.P.; Meggiolaro, M.A. Fatigue Design Techniques, v. 1: High-Cycle Fatigue. CreateSpace, 2016.
- [6] Luong, M. P. Fatigue limit evaluation of metals using an infrared thermographic technique. *Mech Mater* 28:155-163, 1998.
- [7] La Rosa, G.; Risitano, A. Thermographic methodology for rapid determination of the fatigue limit of materials and mechanical components. *Int J Fatigue* 22:65-73, 2000.
- [8] Fargione, G.; Geraci, A.; La Rosa, G.; Risitano, A. Rapid determination of the fatigue curve by the thermographic method. *Int J Fatigue* 24:11-19, 2002.
- [9] Curà, F.; Curti, G.; Sesana, R. A new iteration method for the thermographic determination of fatigue limit of steels. *Int J Fatigue* 27:453-459, 2005.
- [10] Risitano, A.; Risitano, G. Cumulative damage evaluation of steel using infrared thermography. *Theor Appl Fract Mech.* 54:82-90, 2010.
- [11] Hou, P.; Fan, J.; Guo, Q.; Guo, X. The application of the infrared thermography on Ti alloy for studying fatigue behavior. *Frattura ed Integrità Strutturale* 27:21-27, 2014.
- [12] Lipski, A. Thermographic method based accelerated fatigue limit calculation for steel X5CRNI18-10 subjected to rotating bending. *Polish Maritime Res* 22:64-69, 2015.
- [13] Lipski, A. Accelerated determination of the fatigue limit and the S-N curve by means of the thermographic method for X5CrNi18-10 steel. *Acta Mech Autom* 10:22-27, 2016.
- [14] ASTM E466: Standard practice for conducting force controlled constant amplitude axial fatigue tests of metallic materials, ASTM 2015.
- [15] Dixon, WJ. The up-and-down method for small samples. *Am Stat Assoc J* 60(312): 967-978, 1965.

Corresponding author jtcastro@puc-rj.br